Available online at www.sciencedirect.com
ScienceDirect
Journal of the European Ceramic Society 27 (2007) 4537–4546
www.elsevier.com/locate/jeurceramsoc

Influence of synthesis parameters on morphology and phase composition of porous titania layers prepared via water based chemical solution deposition

I. Truijen [a], I. Haeldermans [a], M.K. Van Bael [a,c], H. Van den Rul [a,c], J. D'Haen [b,c], J. Mullens [a,*], H. Terryn [d], V. Goossens [d]

[a] *Hasselt University, Institute for Materials Research, Laboratory of Inorganic and Physical Chemistry, Agoralaan-building D, B-3590 Diepenbeek, Belgium*
[b] *Hasselt University, Institute for Materials Research, Physical Analysis Group, Wetenschapspark 1, B-3590 Diepenbeek, Belgium*
[c] *IMEC vzw, Division IMOMEC, Agoralaan-building D, B-3590 Diepenbeek, Belgium*
[d] *Department of Metallurgy, Electrochemistry and Materials Science, Vrije Universiteit Brussel, Pleinlaan 2, B-1050 Brussels, Belgium*

Received 9 November 2006; received in revised form 31 January 2007; accepted 3 February 2007
Available online 3 April 2007

Abstract

In this work, thick nanocrystalline mesoporous titania layers are synthesized via chemical solution deposition using a water based citratoperoxo-Ti(IV)-precursor solution. The aqueous citratoperoxo-Ti(IV)-precursor solution is modified by the addition of polyvinyl alcohol (PVA), which acts as a thickener and pore forming agent. Layers are tape casted onto ITO-coated glass substrates and are thermally processed. The influence of process parameters like Ti(IV)-concentration, blade thickness, crystallization temperature and time on the film's phase composition, morphology and thickness are investigated by means of X-ray diffraction (XRD), Raman spectroscopy, scanning electron microscopy (SEM), transmission electron microscopy (TEM), variable angle spectroscopic ellipsometry (VASE), atomic force microscopy (AFM) and profilometry.

It is shown that the Ti(IV)-concentration and heat treatment influence the size and shape of the grains of which the films are composed, the film morphology (porosity, surface roughness) and the layer thickness, but no influence on the phase formation is observed. In all cases phase pure anatase layers are obtained.

Keywords: Aqueous synthesis; Films; Sol–gel processes; Tape casting; TiO_2; Porosity

1. Introduction

The potential implementation of nanocrystalline titanium dioxide (TiO_2) layers in applications ranging from photocatalysts[1–5] to photovoltaic cells[5–9] and gas sensors,[10] leads to much effort in trying to develop layers with a mesoporous morphology. Titanium dioxide is favoured for these applications, because it has a high photoactivity, it is biocompatible and chemically inert, readily available and cheap.

Many papers have been published on the preparation of dense TiO_2 layers using various methods such as sputter techniques,[11–16] chemical vapour deposition (CVD)[17–20] and sol–gel synthesis.[8,9,21–23]

The sol–gel route allows a precise control of layer thickness and particle size by optimizing process parameters such as metal ion concentration, deposition thickness, crystallization temperature and time, etc. Moreover, in combination with a chemical solution deposition method large area, high purity films can be produced simply. Due to these advantages, the use of sol–gel synthesis combined with templating methods to prepare mesoporous titania layers, is a very interesting area of study.

Sol–gel methods using templates have been reported for the preparation of titania layers with a mesoporous structure. In these methods ionic and neutral surfactants have been successfully employed.[24,25] Also block copolymers can be used to

* Corresponding author. Tel.: +32 11 26 83 08; fax: +32 11 26 83 01.
E-mail addresses: ine.truijen@uhasselt.be (I. Truijen), marlies.vanbael@uhasselt.be (M.K. Van Bael), heidi.vandenrul@uhasselt.be (H. Van den Rul), jan.dhaen@uhasselt.be (J. D'Haen), jules.mullens@uhasselt.be (J. Mullens), hterryn@vub.ac.be (H. Terryn), vgoossens@vub.ac.be (V. Goossens).

0955-2219/$ – see front matter © 2007 Elsevier Ltd. All rights reserved.
doi:10.1016/j.jeurceramsoc.2007.02.200

direct the formation of mesoporous titania.[26,27] In addition, non-surfactant organic compounds such as polyethylene glycol,[28,29] hydroxypropyl cellulose,[30] diolates[31] and cyclodextrines[32] have been used as pore formers.

In the reported studies mentioned above the traditional sol–gel route, which starts from metal oxides, salts or alkoxides dissolved in alcoholic solvents, is used. In this report however, porous nanocrystalline titania layers are prepared by means of a water based aqueous solution–gel route in combination with tape casting. In previous work, the aqueous solution–gel route has proved to be successful for the preparation of dense titania layers.[33] The reasons for choosing an aqueous route have an obvious economical and environmental basis. Water is less expensive and more environmental friendly than alcoholic solvents. Furthermore, no special precautions to protect the starting products from air or humidity have to be taken. In order to obtain thick porous titania layers, the water based citratoperoxo-Ti(IV)-precursor solution is modified by the addition of polyvinyl alcohol (PVA), which acts as a thickener and pore forming agent.[34] In this study, the influence of the Ti(IV)-concentration, blade thickness and crystallization temperature and time on the layers' thickness, phase composition and morphology is investigated.

2. Experimental

2.1. Materials and reagents

Starting materials for the preparation of the citratoperoxo-Ti(IV)-precursor solution are Ti(IV)-isopropoxide ($Ti(iOPr)_4$, 98+%, Acros), citric acid ($C_6H_8O_7$, 99%, Aldrich), hydrogen peroxide (H_2O_2, 35 wt.% in H_2O, p.a., stabilized, Acros) and ammonia (NH_3, 32% in H_2O, extra pure, Merck). Polyvinyl alcohol (Acros, MW 88,000, 88% hydrolyzed) is used as a thickener and pore forming agent.

2.2. Synthesis of the coating paste

For the preparation of the citratoperoxo-Ti(IV)-precursor solutions with Ti(IV)-concentrations of 0.2, 0.4 and 0.8 M, Ti(IV)-isopropoxide is hydrolyzed in H_2O which leads to the precipitation of a hydroxide. In a next step citric acid and H_2O_2 are added to this precipitate in a 2:1 and 1.2:1 molar ratio against Ti(IV), respectively. Clear, red, stable solutions are obtained. The pH of the resulting citratoperoxo-Ti(IV)-precursor solutions is adjusted to pH 2 using NH_3. More details about the preparation of the citratoperoxo-Ti(IV)-precursor solution are reported elsewhere.[35] In order to deposit thick layers, the viscosity of the original Ti(IV)-precursor solution is increased by addition of an aqueous solution of polyvinyl alcohol (PVA). In a separate container a PVA solution (15 wt.% in water) is prepared by dissolving 6 g PVA in 34 g distilled water, followed by continuous stirring at 70 °C during 10 h. The resulting, clear, polymer solution is added to the citratoperoxo-Ti(IV)-precursor solution in a 1:1 weight ratio. In this way, highly viscous orange coating pastes, containing 7.5 wt.% PVA, are obtained.[34]

2.3. Preparation of the TiO_2 layers

Titania layers are prepared on indium tin oxide (ITO) coated glass substrates (soda lime glass/SiO_2/ITO, 12 Ω/sq ITO, 2.5 cm × 4.0 cm). Prior to deposition, the substrates undergo a cleaning procedure consisting of three steps: an ultrasonic treatment of successively 30 and 10 min in a bath filled with respectively detergent (Ultramet® 2 Sonic Cleaning Solution, Buehler) and acetone (p.a. Acros), followed by a final cleaning step of 10 min in boiling isopropanol (p.a. Acros). Layers are deposited by tape casting (Film Applicator Coatmaster 509 MC, Erichsen Testing Equipment) the coating pastes at room temperature. The speed at which the blade moves forward is set at 80 mm/s and the distance between the blade and substrate (blade thickness) is varied from 30 to 120 μm. Next, all layers are sub-

Table 1
Preparation conditions and properties of thick TiO_2 layers

Sample	Ti^{4+}-concentration (M)	Crystallization temperature (°C) and time (min.)	Blade thickness (μm)	Number of deposited layers	Film thickness		Rms surface roughness (nm)
					nm*	μm**	
A1	0.2	450, 180	90	1	628 ± 27	/	76
A2	0.2	450, 180	90; 90	2	421 ± 19	0.40-0.50	88
A3	0.2	600, 60	90	1	224 ± 13	0.20	16
A4	0.2	600, 60	120	1	334 ± 33	0.28	19
B1	0.4	450, 180	90	1	610 ± 66	0.60	122
B2	0.4	450, 180	90; 90	2	1205 ± 16	1.10	108
B3	0.4	600, 60	90	1	403 ± 7	0.38	62
B4	0.4	600, 60	120	1	580 ± 11	0.65	81
C1	0.8	450, 120	90	1	783 ± 61	0.62	25
C2	0.8	450, 180	90	1	824 ± 26	0.75	28
C3	0.8	450, 180	90; 60	2	1075 ± 77	1.01	60
C4	0.8	450, 180	90; 90	2	1480 ± 108	1.37	33
C5	0.8	600, 60	30	1	276 ± 58	0.20	2.4
C6	0.8	600, 60	60	1	410 ± 41	0.38	2.6
C7	0.8	600, 60	90	1	530 ± 26	0.50	1.7
C8	0.8	600, 60	120	1	Cracks	Cracks	Cracks

Film thicknesses are measured by means of profilometry* and cross sectional SEM**. With the latter the attainable detail is 0.01 μm.

jected to a drying step of 20 min at 60 °C in a furnace under flowing air. The samples are finally placed in a horizontal tube oven and heated in dry air at a heating rate of 5 °C/min from room temperature up to 450 or 600 °C, followed by an isothermal step at these temperatures of respectively 120 or 180 (at 450 °C) and 60 min (at 600 °C). For convenience, all samples are numbered and listed in Table 1.

2.4. Characterization techniques

The formation of crystalline phases in the samples upon heating is studied at room temperature by X-ray diffraction (XRD) using a Siemens D-5000 diffractometer with Cu Kα1 radiation and by Raman spectrometry using a Renishaw inVia Reflex RAMAN spectrometer (Argon laser: 514.5 nm) with a Leica DMLM optical microscope. Scanning electron micrographs of the layers are obtained on a Philips XL30-FEG SEM and on a FEI Quanta 200FEG-SEM, both equipped with secondary electron (SE) and back scattered electron (BSE) detectors. After removal of the underlying glass substrate by etching with a 40 vol.% aqueous HF solution, transmission electron microscopic (TEM) images of the resulting free standing films are made on a Philips CM12-STEM. RMS surface roughnesses are measured by atomic force microscopy (AFM) using an Autoprobe CP from Park Scientific Instruments under ambient atmosphere. The measurements are performed in a non-contact mode using an etched silicon tip (Ultrasharp MikroMash NSC11 B). Scan sizes of 2 μm × 2 μm and 4 μm × 4 μm are used. Variable angle spectroscopic ellipsometry (VASE) is carried out at room temperature on a Woollam VASE UV-VIS-NIR apparatus. The ellipsometric angles Ψ and Δ are measured in a spectral range of 300–1700 nm with a wavelength resolution of 10 nm at three angles of incident, 65°, 70° and 75°. The ellipsometric data are analyzed using the WVASE32 version 3.486 software package developed by J.A. Woollam Co. Because, the complex substrate layer stack (glass/ITO/TiO_2) of the samples hinders the model definition, for these measurements comparable layers are prepared on borosilicate glass (glass/TiO_2).

Layer thicknesses are determined by means of cross sectional SEM (X-SEM) and profilometry (Sloan Dektak[3] Surface Profiler). For the latter, scratches are made at five different locations on the film. A small accumulation of material is seen along the borders of these scratches. Therefore, step heights are measured between the bottom of the scratch and the plateau just aside the accumulation, assuming that the plateau is completely flat. A mean value for the film thickness is calculated.

3. Results and discussion

3.1. The effect of the Ti(IV)-concentration and crystallization temperature on the phase formation

XRD spectra (Fig. 1a) of layers obtained from 7.5 wt.% PVA 0.2 M (A1); 0.4 M (B1) and 0.8 M (C2) citratoperoxo-Ti-precursor pastes and crystallized at 450 °C for 3 h, indicate that phase pure anatase films are formed at this crystallization temperature. No diffraction peaks of the rutile crystalline phase are

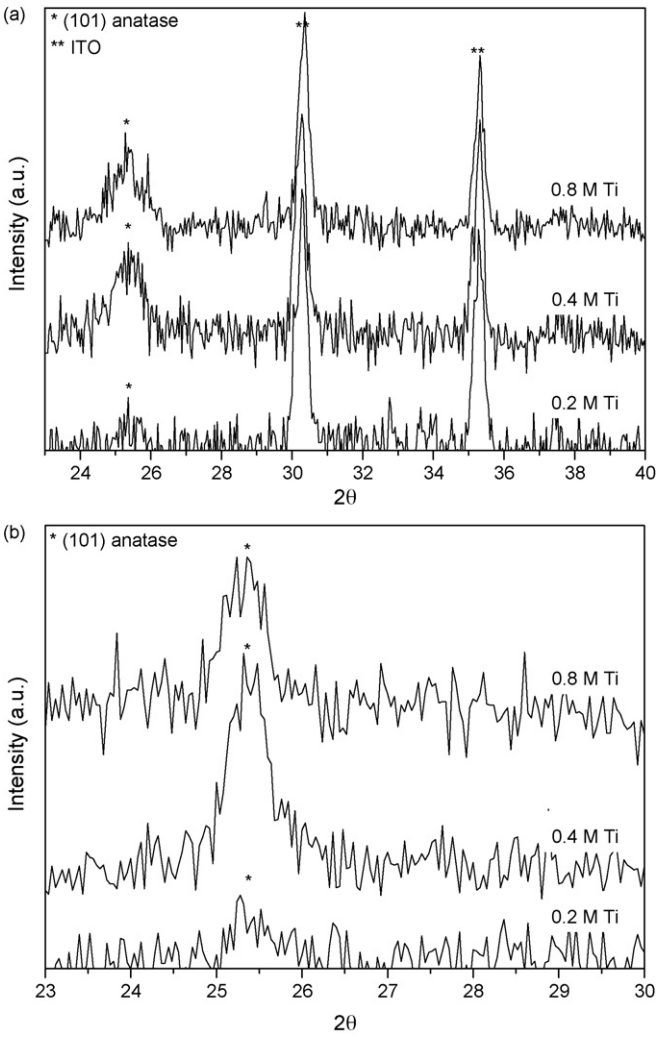

Fig. 1. Powder X-ray diffraction spectra (XRD) of TiO_2 layers obtained from 7.5 wt.% PVA citratoperoxo-Ti(IV)-precursor solutions with different Ti^{4+}-concentrations (0.2, 0.4, and 0.8 M) crystallized at: (a) 450 °C during 180 min (A1, B1, and C2); (b) 600 °C during 60 min (A3, B3, and C7).

observed. In spite of the fact that the anatase diffraction peak is very broad and the difference between the *d*-values of anatase ((1 0 1), 25.28°, 2θ) and brookite ((2 1 0), 25.36°, 2θ) is very small, the presence of brookite can be excluded because of the absence of an intense diffraction peak at 30.83°, 2θ, assuming that there is no preferential orientation. The XRD spectra further reveal the presence of two intense diffraction peaks at 30.56°, 2θ and 35.34°, 2θ, which can be assigned to the underlying indium tin oxide coating.

Also crystallization at 600 °C during 1 h results in the formation of phase pure anatase layers (Fig. 1b). However, the intensity of the TiO_2 peaks is very low. This can be attributed to the fact that there is too few material present in the layers. In order to give a decisive answer about the absence of the brookite and rutile crystalline phases in the layers crystallized at 450 and 600 °C additional Raman measurements are performed. Fig. 2 shows the Raman spectra for both layers. Five well-defined peaks appear around 144, 199, 398, 519 and 637 cm^{-1}. Including the superposition of two peaks near 519 cm^{-1}, these six peaks correspond

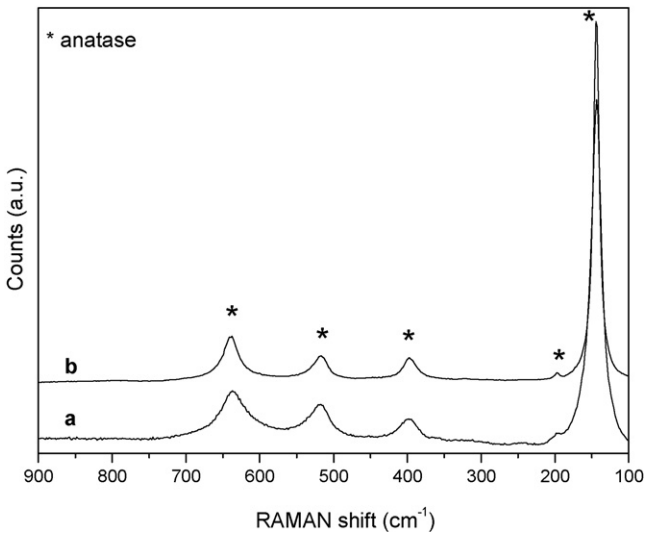

Fig. 2. Raman spectra of TiO_2 layers obtained from a 7.5 wt.% PVA 0.8 M citratoperoxo-Ti(IV)-precursor solution crystallized at (a) 450 °C during 180 min (C2) and (b) 600 °C during 60 min (C7).

to the six fundamental vibrational modes of anatase with the symmetries of E_g, E_g, B_{1g}, A_{1g}, B_{1g}, and E_g, respectively.[36] The positions and intensities of the five Raman active modes are in accordance with the values reported in literature.[36–38] Fundamental vibrational modes of rutile and brookite[36] do not appear in the spectra shown in Fig. 2. Hereby, the assumption made by XRD that phase pure anatase layers are obtained after crystallization at 450 or 600 °C, is confirmed.

The absence of the rutile crystalline phase in the sample crystallized at 600 °C is in contrast with the phase composition of a layer deposited out of a 0.4 M citratoperoxo-Ti(IV)-precursor solution without PVA and crystallized at 600 °C. XRD-data of the latter illustrate that both the anatase and rutile crystalline phase are present.[33] These results indicate the influence of polyvinyl alcohol on the phase formation, although the underlying process is still an unsolved issue.

Both the Ti(IV)-concentration and crystallization temperature show no effect on the phase composition. In all cases, phase pure anatase layers are obtained. The absence of rutile in the layers studied in this work, is very interesting with respect to their application in dye-sensitized solar cells. In these devices an as high as possible fraction of anatase is desired, since this crystallographic phase has the advantage of transporting electrons with higher efficiency.[5,39]

3.2. The effect of the Ti(IV)-concentration, crystallization temperature and time on the film morphology

The influence of crystallization temperature and time on the morphology of the titania layers is also studied. TEM analysis performed on films previously stripped of from their substrates (samples C1, C2 and C7) reveals (Fig. 3) that both crystallization time and temperature affect the size of the particles in the films. A longer crystallization time (180 min at 450 °C) or a higher crystallization temperature (600 °C) leads to an increase of the grain sizes. As shown in Fig. 3a, grain dimensions are very small in sample C1, crystallized at 450 °C during 120 min, which makes it impossible to determine primary particle sizes. However, when crystallized at this temperature during 180 min, spherical grains of about 10 nm can be distinguished (Fig. 3b). Furthermore, a crystallization temperature of 600 °C results in a small grain growth and a larger size distribution due to the additional formation of some larger grains. The latter can be very interesting regarding the implementation of the layers in a dye-sensitized solar cell, because the presence of some larger particles enhances scattering of the incident light and therefore also the probability of the photon to interact with a dye molecule,[39,40] and thus the efficiency of the solar cell.

Based on the intensity of the diffraction rings in the electron diffraction patterns of the samples C1, C2 and C7 we can conclude that crystallinity and grain size in the films increases with increasing crystallization temperature and time.

According to TEM analysis, the same conclusions concerning the effect of crystallization temperature on the grain size can be made for samples obtained from the 0.2 and 0.4 M Ti(IV)-precursor pastes (Fig. 4). However, in contrast to higher Ti(IV)-concentrations (0.4 and 0.8 M) which give rise to the formation of spherical grains, particles with irregular shapes are observed when using a 0.2 M Ti(IV)-concentration (Fig. 4b). This can possibly be explained by the nucleation mechanism of the grains. At low Ti(IV)-concentrations few nuclei which show different growth rates and directions originate in the solution upon

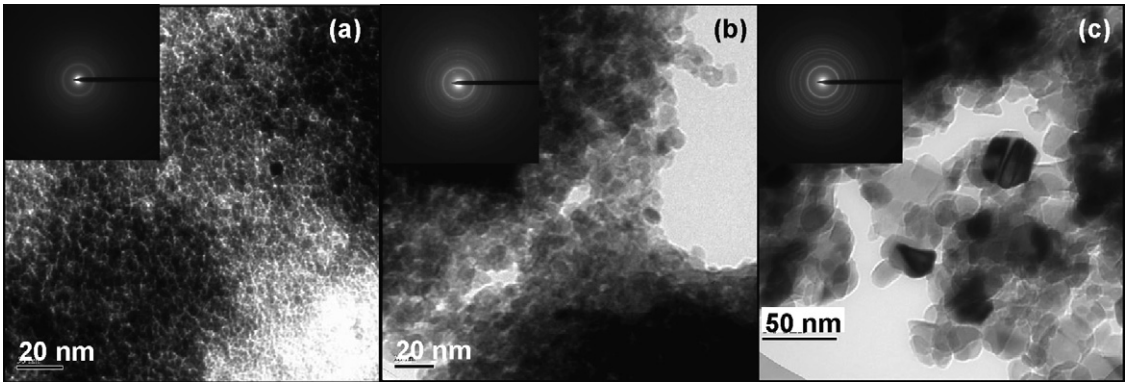

Fig. 3. TEM images and electron diffraction patterns of TiO_2 layers obtained from a 0.8 M citratoperoxo-Ti(IV)-precursor solution: (a) crystallized at 450 °C during 120 min (C1); (b) crystallized at 450 °C during 180 min (C2); (c) crystallized at 600 °C during 60 min (C7).

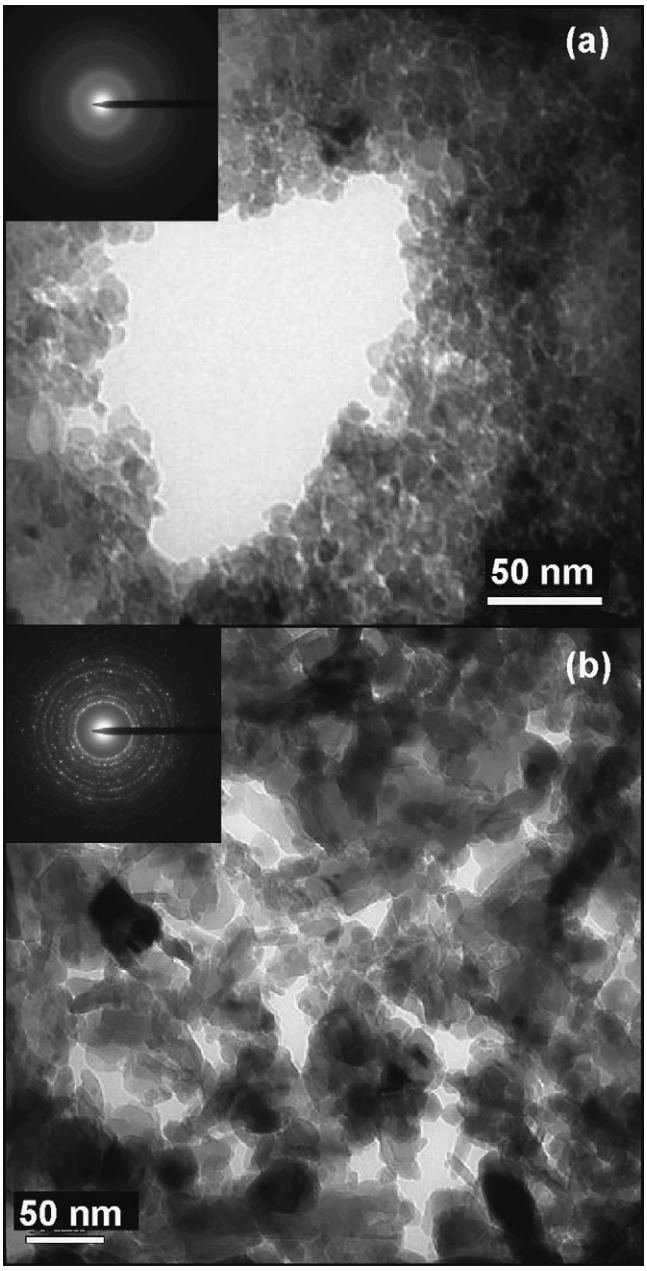

Fig. 4. TEM images and electron diffraction patterns of TiO_2 layers obtained from: (a) a 0.4 M citratoperoxo-Ti(IV)-precursor solution and crystallized at 450 °C during 180 min (B1); (b) a 0.2 M citratoperoxo-Ti(IV)-precursor solution crystallized at 600 °C during 60 min (A3).

heating, resulting in particles with different shapes and sizes. However, at high concentrations a great amount of nuclei with the same shape and size, which grow simultaneously, are formed.

Cross sectional SEM analysis (Fig. 5) points out that by deposition of a coating paste with higher Ti(IV)-concentration (0.8 M) layers with a more uniform layer thickness are obtained. Moreover, a higher crystallization temperature (600 °C) improves the uniformity of all layers. Inhomogeneity of the low Ti(IV)-concentration samples can possibly be explained by the fact that the wet layers contain a lower Ti(IV) to PVA ratio, so relatively more PVA has to be burned out in these samples. Consequently, deposition of uniform layers by means of tape casting is more difficult when using a precursor paste with a low Ti(IV)-concentration.

In accordance with the above results, the same influence of Ti(IV)-concentration and crystallization temperature is seen on the rms roughness of the layers. By means of AFM no linear trend in rms roughness is observed, but it is proved that the highest Ti(IV)-concentration and/or highest crystallization temperature result in the formation of smoother layers (Table 1). For sample C7 an rms roughness of only 1.7 nm is observed. The effect of crystallization temperature on the layers' roughness is also observed with SEM. Samples crystallized at 450 °C (Fig. 6a–d) exhibit a more rough and porous surface than those crystallized at 600 °C. In contrast to the layers treated at 450 °C, the C7 layer crystallized at 600 °C shows a much smoother surface, containing clearly defined pores of 20 nm, homogenously distributed along the surface (Fig. 6f). According to cross sectional SEM analysis (Fig. 7), the 600 °C crystallized sample seems a little less porous than the layers treated at 450 °C.

In literature different kinds of techniques are reported to study the porous characteristics of powders.[41–43] However, quantification of the layers' porosity has proven to be a difficult issue. To get an idea of the porosity, the pore size and the pore size distribution of our TiO_2 layers, several techniques are investigated. A first one is N_2-sorption porosimetry. Regarding this technique a specific problem with respect to the detection limit of the apparatus raises. It appears that there is too few material on top of the substrate and therefore a low signal/noise ratio is obtained.[44]

When using image analysis to study the porous properties of the layers an insufficient contrast between the ceramic material and the substance in the pores, makes it impossible to extract meaningful information starting from an SEM image.

However, with spectroscopic ellipsometry we are able to obtain a value for the porosity of the layers. The ellipsometric spectra of the layers crystallized at 450 and 600 °C are shown in Fig. 8. To extract the refractive index from these data the titania layers are modelled using a Cauchy dispersion relationship (see Eq. (1)), implying the transparency of the layers. To account for a low absorption in the UV region Eq. (2) is used in the model (Urbach tail).

$$n(\lambda) = A_n + B_n/\lambda^2 \quad (1)$$

$$k(\lambda) = A_k\, e^{\beta(12{,}400((1/\lambda)-(1/\gamma)))} \quad (2)$$

The model is built of parallel layers showing a flat interface. Every single layer is characterized by its layer thickness and optical constants. The optical constants of the substrates are calculated separately and are inserted in the model.

Ellipsometric spectra are calculated and fitted to the experimental data using the film thickness, A_n, B_n (Cauchy parameters), A_k and β (Urbach tail) as fit parameters. The non-uniformity of the film is also fitted to account for the variation in the thickness of the film on the substrate. As criterion to determine the accuracy of the optical model, the mean squared error (MSE) between the experimental and the fitted data is used.[45] The MSE values obtained for the 450 and 600 °C sample are 3.824 and 2.226. According to these low values it can be

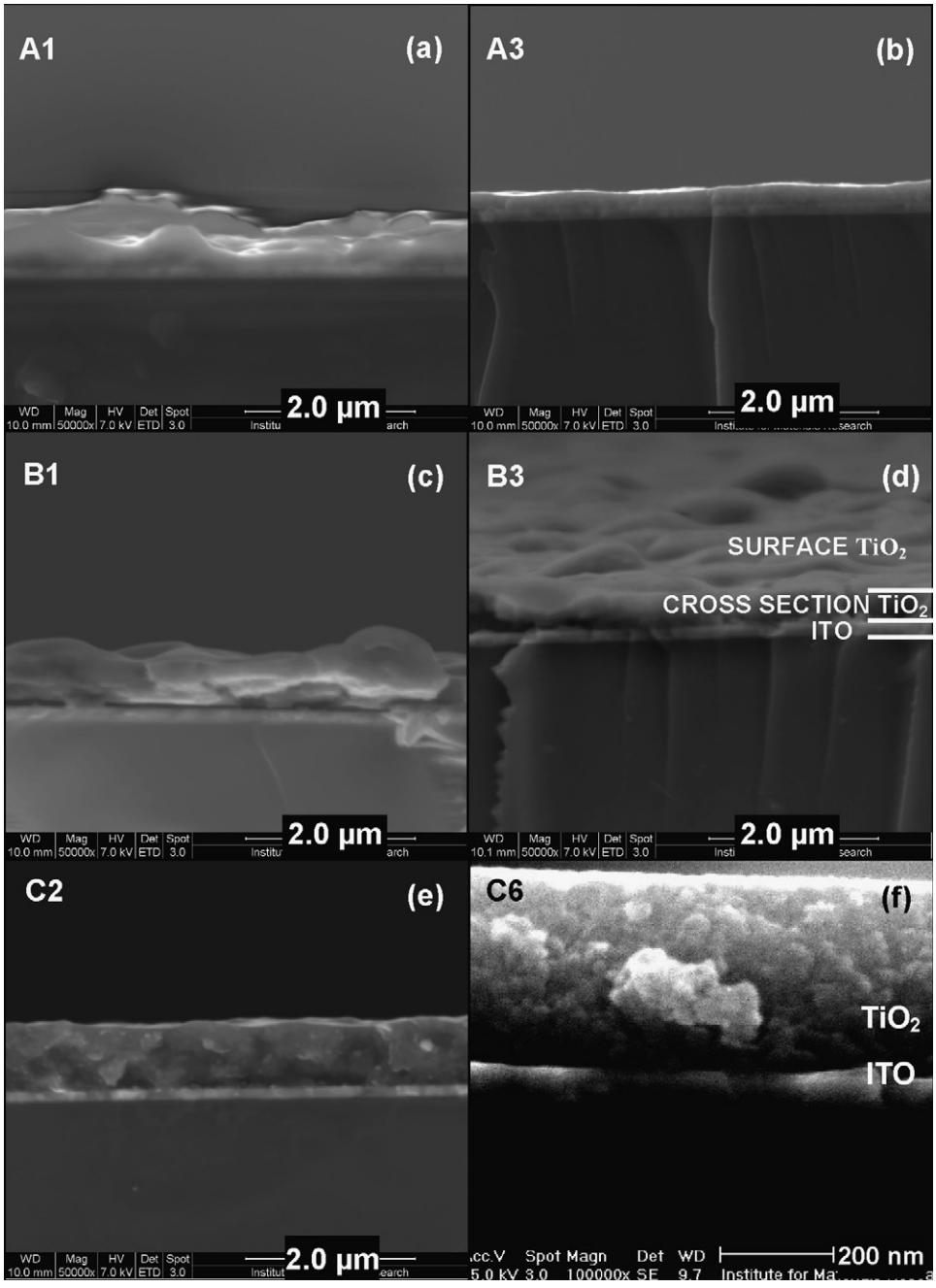

Fig. 5. Cross-section SE SEM images of TiO_2 layers obtained from: a 0.2 M citratoperoxo-Ti(IV)-precursor solution and crystallized at (a) 450 °C during 180 min (A1); (b) at 600 °C during 60 min (A3), a 0.4 M citratoperoxo-Ti(IV)-precursor solution and crystallized at (c) 450 °C during 180 min (B1); (d) at 600 °C during 60 min (B3), a 0.8 M citratoperoxo-Ti(IV)-precursor solution and crystallized at (e) 450 °C during 180 min (C2); (f) at 600 °C during 60 min (C6).

stated that our model indeed produces values which resemble the experimental values closely.

Values of porosity are calculated by using Eq. (3).[46] n is the refractive index of the layers obtained with spectroscopic ellipsometry at 550 nm. n_0 is the refractive index of bulk anatase at 550 nm (2.54).[15]

$$P = 100 \times \left[1 - \frac{n^2 - 1}{n_0^2 - 1}\right] \quad (3)$$

The layers heat treated at 450 and 600 °C show a porosity of 46 and 42%, respectively. This confirms the conclusion drawn from cross sectional SEM analysis that the 600 °C crystallized samples are only a little less porous than the layers treated at 450 °C.

The lower porosity of the titania layers crystallized at 600 °C can be attributed to particle growth and layer densification at higher temperature. As shown in Fig. 6f, neck formation between the particles is observed. Also, this feature is very interesting with respect to the application of the layer in a dye-sensitized

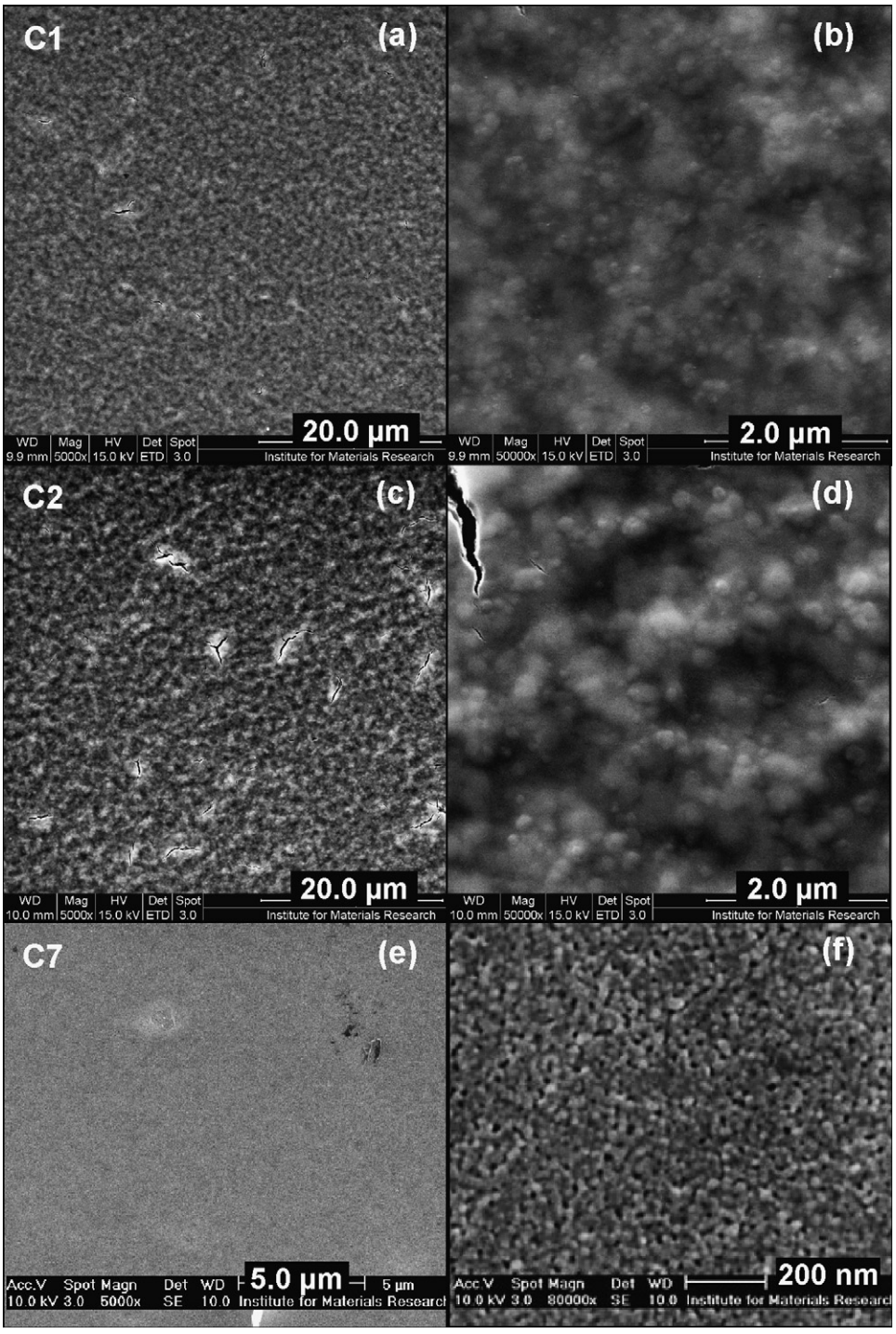

Fig. 6. Plane view SE SEM images of TiO_2 layers obtained from a 0.8 M citratoperoxo-Ti(IV)-precursor solution and crystallized at (a and b) 450 °C during 120 min (C1); (c and d) at 450 °C during 180 min (C2); (e and f) 600 °C during 60 min (C7).

solar cell, which demands a good electron transport throughout the whole titania layer.

3.3. Influence of synthesis parameters on the layer thickness

In this work, mean layer thicknesses are determined by means of profilometry. In order to confirm the thicknesses obtained with profilometry cross sectional SEM is performed on the layers. An accuracy of 0.01 μm can be obtained with this technique. The results obtained with profilometry and cross sectional SEM are in good agreement with each other (Table 1). To study the influence of the blade thickness on the resulting thickness of titania layers crystallized at 600 °C, a 0.8 M Ti(IV) coating paste is tape casted using a blade thickness varying from 30 to 120 μm (C5–C8). As shown in Fig. 9 thickness rises linearly with increasing blade thickness. For the layers deposited using

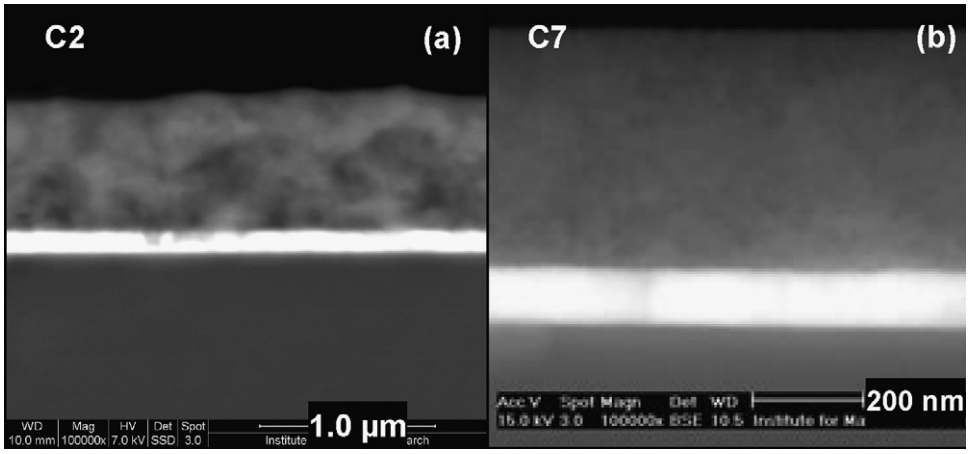

Fig. 7. Cross-section BSE SEM images of TiO_2 layers obtained from a 0.8 M citratoperoxo-Ti(IV)-precursor solution and crystallized at (a) 450 °C during 180 min (C2); (b) at 600 °C during 60 min (C7).

a 120 μm blade thickness, crack formation and flaking off from the substrates is observed. These phenomena can be explained by the fact that inherent to the wet gel film thickness, the amount of organic compounds in the layer increases. In this way large amounts of gas are released simultaneously during thermal treatment, causing the formation of cracks. This problem is also seen by Srikanth et al.[47] They report development of cracks when the PEG content in their titania sol increases. Applying lower heating rates in order to obtain a more gradual precursor decomposition, does not offer a solution for our cracking problem. So a maximum layer thickness of about 500 nm can be obtained at 600 °C.

For the samples deposited using a 90 μm blade thickness also the influence of crystallization temperature on the resulting

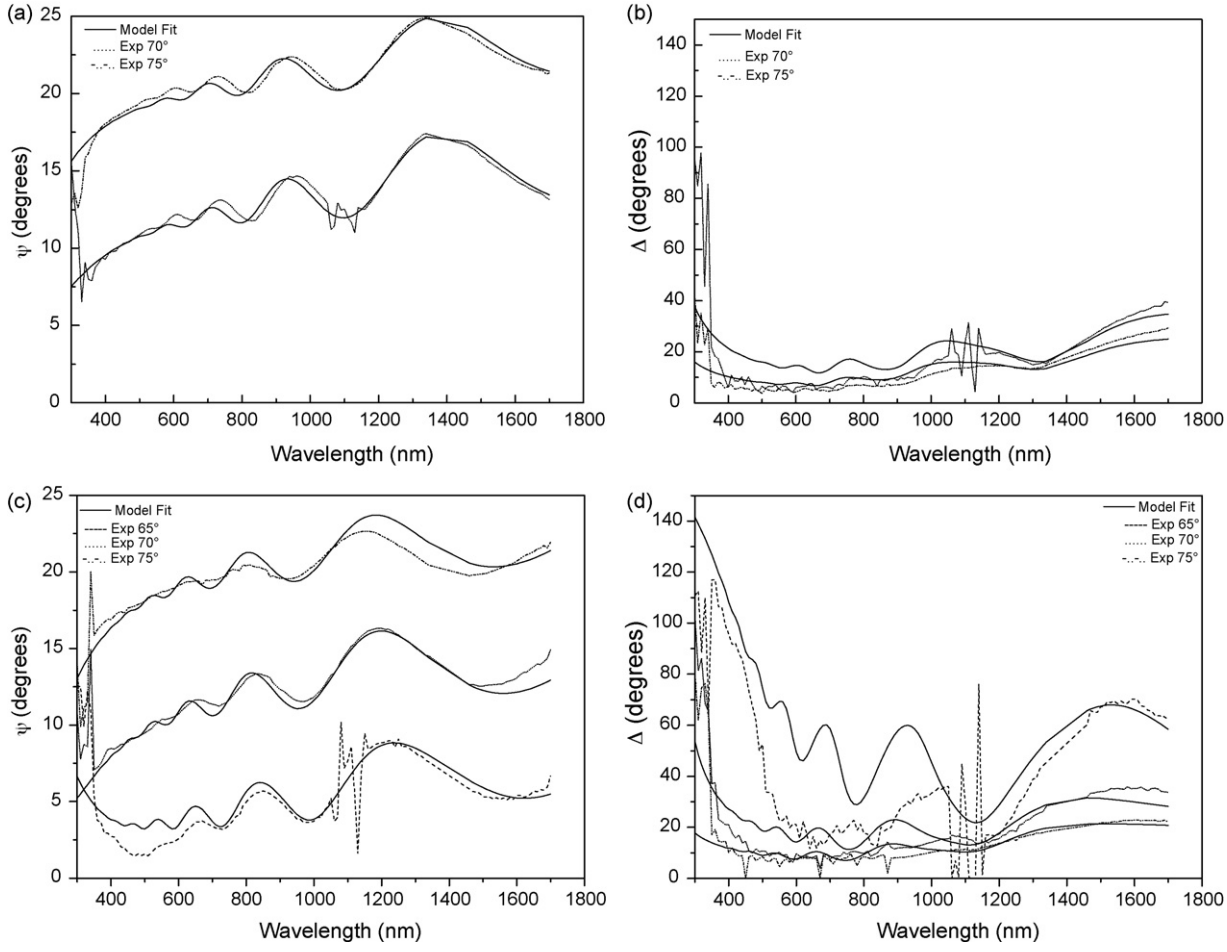

Fig. 8. Ellipsometric spectra for a titania layer crystallized at 450 °C: (a) amplitude change and (b) phase change; 600 °C: (c) amplitude change and (d) phase change.

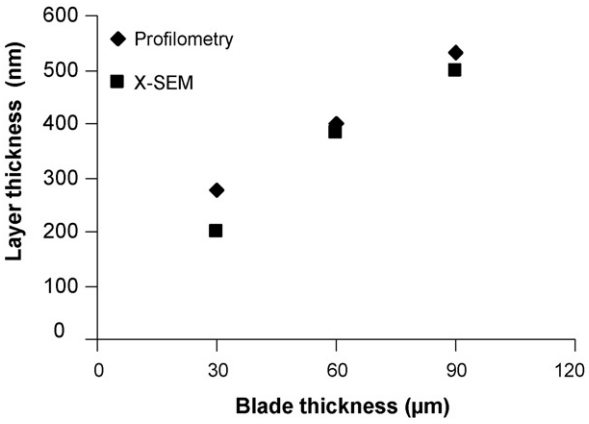

Fig. 9. Film thickness vs. blade thickness determined by cross sectional SEM and profilometry.

layer thickness is investigated. Table 1 shows that this temperature clearly affects the layer thickness. Crystallization at 450 °C results in an anatase layer with a thickness of approximately 800 nm, which is comparable with the thickness observed bij Miki et al.[29] They report about a titania layer with a thickness of 1 μm, obtained by a one run dip coating of an aqueous TiO_2 sol containing PEG.

According to thermogravimetric analysis of the coating paste,[48] the organic matrix is completely removed at 450 °C. Therefore, reduction of layer thickness at 600 °C can only be attributed to layer densification, which confirms the conclusion, drawn from SEM analysis and ellipsometry, that the layers treated at 450 °C are a little bit more porous.

While the glass substrates bend after crystallization at 600 °C, they remain completely flat after thermal treatment at 450 °C. This makes subsequent layer deposition possible. In this way, layer thicknesses can be increased to about 1400 nm by deposition of a second layer, which is also thermally processed at 450 °C during 180 min.

Also, the effect of Ti(IV)-concentration on the layer thickness is presented in Table 1. An increasing Ti(IV)-concentration results in an increasing thickness.

Aiming at the preparation of thick titania layers, only large blade thicknesses (90 and 120 μm) are used for deposition of the low Ti(IV)-concentration coating pastes.

As shown in Table 1, a range of film thicknesses can be prepared by adjusting the blade thickness and/or Ti(IV)-concentration.

4. Conclusion

It is shown that the PVA templated aqueous solution–gel method, presented in this study, enables the preparation of thick, porous, nanocrystalline TiO_2 films, that do not flake off from the substrates. Therefore, this method is an environmentally friendly and simple alternative for its alcoholic counterparts.

This study reveals that layers showing the most potential for implementation in dye-sensitized solar cells are obtained by using a high Ti(IV)-concentration coating paste (0.8 M). In contrast to the low Ti(IV)-concentration coating pastes, tape casting and thermal treatment of a 7.5 wt.% PVA containing 0.8 M citratoperoxo-Ti(IV) coating paste results in the formation of homogeneous titania layers, showing low rms surface roughnesses. It is shown that crystallization temperature clearly affects grain size, film morphology and layer thickness. Crystallization of the 0.8 M Ti(IV) coating paste at lower temperature (450 °C) results in the formation of more porous, thicker (1400 nm) nanocrystalline titania layers, composed of primary particles of about 10 nm. However, at higher crystallization temperature (600 °C) a small grain growth and a larger size distribution is observed. The latter is interesting with respect to the enhanced scattering of the incident light.

XRD and Raman data illustrate that in all cases phase pure anatase layers are formed. This crystallographic titania phase has the advantage of transporting electrons with higher efficiency.

Further investigations concerning the performance of the layers in photovoltaics are now in progress.

Acknowledgements

M. K. Van Bael is a post-doctoral fellow of the Research Foundation Flanders, Belgium (FWO Vlaanderen). The authors would like to thank O. Douhéret and B. Ruttens of the Institute for Materials Research (IMO, UHasselt) for performing the AFM and SEM measurements and RENISHAW (M. Belleil) for performing the Raman experiments.

References

1. Fujishima, A., Rao, T. N. and Tryk, D. A., Titanium dioxide photocatalysis. *J. Photochem. Photobiol. C*, 2000, **1**, 1–21.
2. Kemmitt, T., Al-Salim, N. I., Waterland, M., Kennedy, V. J. and Markwitz, A., Photocatalytic titania coatings. *Curr. Appl. Phys.*, 2004, **4**(2–4), 189–192.
3. Zhao, L., Yu, Y., Song, L., Hu, X. and Larbot, Synthesis and characterization of nanostructured titania film for photocatalysis. *Appl. Surf. Sci.*, 2005, **239**(3/4), 285–291.
4. Mellott, N. P., Durucan, C., Pantano, C. G. and Gugliemi, M., Commercial and laboratory prepared titanium dioxide thin films for self-cleaning glasses: photocatalytic performance and chemical durability. *Thin Solid Films*, 2006, **502**(1/2), 112–120.
5. Carp, O., Huisman, C. L. and Reller, A., Photoinduced reactivity of titanium dioxide. *Prog. Solid State Chem.*, 2004, **32**(1/2), 33–177.
6. Gratzel, M., Sol–gel processed TiO_2 films for photovoltaic applications. *J. Sol–Gel Sci. Technol.*, 2001, **22**(1/2), 7–13.
7. Gratzel, M., Conversion of sunlight to electric power by nanocrystalline dye-sensitized solar cells. *J. Photochem. Photobiol. A-Chem.*, 2004, **164**(1–3), 3–14.
8. Grant, C. D., Schwartzberg, A. M., Smestad, G. P., Kowalik, J., Tolbert, L. M. and Zhang, J. Z., Optical and electrochemical characterization of poly (3-undecyl-2.2'-bithiophene) in thin film solid state TiO_2 photovoltaic solar cells. *Synth. Met.*, 2003, **132**(2), 197–204.
9. Smestad, G. P., Spiekermann, S., Kowalik, J., Grant, C. D., Schwartzberg, A. M., Zhang, J. *et al.*, A technique to compare polythiophene solid-state dye sensitized TiO_2 solar cells to liquid junction devices. *Sol. Energy Mater. Sol. Cells*, 2003, **76**(1), 85–105.
10. Skubal, L. R., Meshkov, N. K. and Vogt, M. C., Detection and identification of gaseous organics using a TiO_2 sensor. *J. Photochem. Photobiol. A-Chem.*, 2002, **148**(1–3), 103–108.
11. Hill, R., Reactive sputtering and the use of anodes for optical coatings. *J. Non-Cryst. Solids*, 1997, **218**, 54–57.
12. Mardare, D. and Hones, P., Optical dispersion analysis of TiO_2 thin films based on variable-angle spectroscopic ellipsometry measurements. *Mater. Sci. Eng. B*, 1999, **68**(1), 42–47.

13. Mardare, D., Baban, C., Gavrila, R., Modreanu, M. and Rusu, G. I., On the structure, morphology and electrical conductivities of titanium oxide thin films. *Surf. Sci.*, 2002, **507**, 468–472.
14. Yamagishi, M., Kuriki, S., Song, P. K. and Shigesato, Y., Thin film TiO_2 photocatalyst deposited by reactive magnetron sputtering. *Thin Solid Films*, 2003, **442**(1/2), 227–231.
15. Boudaden, J., Ho, R. S. C., Oelhafen, P., Schüler, H., Roecker, C. and Scartezzini, J. L., Towards coloured glazed thermal solar collectors. *Sol. Energy Mater. Sol. Cells*, 2004, **84**(1–4), 225–239.
16. Karunagaran, B., Kim, K., Mangalaray, D., Yi, J. and Velumani, S., Structural optical and Raman scattering studies on DC magnetron sputtered titanium dioxide thin films. *Sol. Energy Mater. Sol. Cells*, 2005, **88**(2), 199–208.
17. Mills, A., Elliott, N., Parkin, I. P., O'Neill, S. A. and Clark, R. J., Novel TiO_2 CVD films for semiconductor photocatalysis. *J. Photochem. Photobiol. A-Chem.*, 2002, **151**(1–3), 171–179.
18. Kang, M., Lee, J. H., Lee, S. H., Chung, C. H., Yoon, K. J., Ogino, K. *et al.*, Preparation of TiO_2 film by the MOCVD method and analysis for decomposition of trichloroethylene using in situ FT-IR spectroscopy. *J. Mol. Catal. A-Chem.*, 2003, **193**(1/2), 273–283.
19. Jung, C. K., Lee, S. B., Boo, J. H., Ku, S. J., Yu, K. S. and Lee, J. W., Characterization of growth behavior and structural properties of TiO_2 thin films grown on Si(1 0 0) and Si(1 1 1) substrates. *Surf. Coat. Technol.*, 2003, **174/175**, 296–302.
20. Backman, U., Auvinen, A. and Jokiniemi, J. K., Deposition of nanostructured titania films by particle-assisted MOCVD. *Surf. Coat. Technol.*, 2005, **192**(1), 81–87.
21. Fan, Q., McQuillin, B., Ray, A. K., Turner, M. L. and Seddon, A. B., High density, non-porous anatase titania thin films for device applications. *J. Phys. D-Appl. Phys.*, 2000, **33**(21), 2683–2686.
22. Tracey, S. M., The role and interactions of process parameters on the nature of alkoxide derived sol–gel films. *J. Mater. Process. Technol.*, 1998, **77**, 86–94.
23. Kishimoto, T. and Kozuka, H., Sol–gel preparation of TiO_2 ceramic coating films from aqueous solutions of titanium sulfate (IV) containing polyvinylpyrrolidone. *J. Mater. Res.*, 2003, **18**(2), 466–474.
24. Hirashima, H., Imai, H., Miah, M. Y., Bountseva, I. M., Beckman, I. N. and Balek, V., Preparation of mesoporous titania gel films and their characterization. *J. Non-Cryst. Solids*, 2004, **350**, 266–270.
25. Cassiers, K., Linssen, T., Mathieu, M., Bai, Y. Q., Zhu, H. Y., Cool, P. *et al.*, Surfactant-directed synthesis of mesoporous titania with nanocrystalline anatase walls and remarkable thermal stability. *J. Phys. Chem. B*, 2004, **108**(12), 3713–3721.
26. Kitazawa, N., Sakaguchi, K., Aono, M. and Watanabe, Y., Synthesis of mesostructured titanium dioxide films by surfactant-templated sol–gel method. *J. Mater. Sci.*, 2003, **38**(14), 3069–3072.
27. Yun, H. S., Miyazawa, K., Honma, I., Zhou, H. and Kuwabara, M., Synthesis of semicrystallized mesoporous TiO_2 thin films using triblock copolymer templates. *Mater. Sci. Eng. C*, 2003, **23**(4), 487–494.
28. Guo, B., Liu, Z. L., Hong, L., Jiang, H. and Lee, J. Y., Photocatalytic effect of the sol–gel derived nanoporous TiO_2 transparent thin films. *Thin Solid Films*, 2005, **479**(1/2), 310–315.
29. Miki, T., Nishizawa, K., Suzuki, K. and Kato, K., Preparation of thick TiO_2 film with large surface area using aqueous sol with poly(ethylene glycol). *J. Mater. Sci.*, 2004, **39**(2), 699–701.
30. Zhao, G., Tian, Q., Liu, Q. and Han, G., Effects of HPC on the microstructure and hydrophilicity of sol–gel-derived TiO_2 films. *Surf. Coat. Technol.*, 2005, **198**(1–3), 55–58.
31. Thoms, H., Epple, M., Fröba, M., Wong, J. and Reller, A., Metal diolates: useful precursors for tailor-made oxides prepared at low temperatures. *J. Mater. Chem.*, 1998, **8**(6), 1447–1451.
32. Zheng, J. Y., Pang, J. B., Qiu, K. Y. and Wei, Y., Synthesis of mesoporous titanium dioxide materials by using a mixture of organic compounds as a non-surfactant template. *J. Mater. Chem.*, 2001, **11**(12), 3367–3372.
33. Truijen, I., Van Bael, M. K., Van den Rul, H., D'Haen, J. and Mullens, J., Synthesis of thin dense titania films via an aqueous solution–gel method. *J. Sol–Gel Sci. Technol.*, 2007, **41**(1), 43–48.
34. Truijen, I., Van Bael, M. K., Van den Rul, H., D'Haen, J. and Mullens, J., Preparation of nanocrystalline titania films with different porosity by water based chemical solution deposition; submitted.
35. Van Werde, K., Vanhoyland, G., Nelis, D., Mondelaers, D., Van Bael, M. K., Mullens, J. *et al.*, Phase formation of ferroelectric perovskite 0.75 Pb(Zn-1/3.Nb-2/3)O-3-0. 25 $BaTiO_3$ prepared by aqueous solution-gel chemistry. *J. Mater. Chem.*, 2001, **11**(4), 1192–1197.
36. Tompsett, G. A., Bowmaker, G. A., Cooney, R. P., Metson, J. B., Rodgers, K. A. and Seakins, J. M., The Raman spectrum of Brookite, TiO_2 (PBCA $Z = 8$). *J. Raman Spectrosc.*, 1995, **26**(1), 57–62.
37. Miao, L., Tanemura, S., Toh, S., Kaneko, K. and Tanemura, M., Fabrication characterization and Raman study of anatase TiO_2 nanorods by a heating-sol–gel template process. *J. Cryst. Growth*, 2004, **264**(1–3), 246–252.
38. Baia, L., Peter, A., Cosoveanu, V., Indea, E., Baia, M., Popp, J. *et al.*, Synthesis and nanostructural characterization of TiO_2 aerogels for photovoltaic devices. *Thin Solid Films*, 2006, **511**, 512–516.
39. Tsukahara, J., Shiratsuchi, K., Kubota, T. and Sen, S., European Patent 1.107.333 A2, 13 June 2001.
40. Barbé, C. J., Arendse, F., Comte, P., Jirousek, M., Lenzmann, F., Shklover, V. *et al.*, Nanocrystalline titanium oxide electrode for photovoltaic applications. *J. Am. Ceram. Soc.*, 1997, **80**(12), 3157–3171.
41. Rouquerol, J., Avnir, D., Fairbridge, C. W., Everett, D. H., Haynes, J. H., Pernicone, N. *et al.*, Recommendations for the characterization of porous solids. *Pure Appl. Chem.*, 1994, **66**(8), 1739–1758.
42. Sing, K. S. W., Characterization of porous materials: past, present and future. *Colloids Surf. A*, 2004, **241**(1–3), 3–7.
43. Denoyel, R., Llewellyn, P., Beurroies, I., Rouquerol, J., Rouquerol, F. O. and Luciani, L., Comparing the basic phenomena involved in three methods of pore-size characterization: gas adsorption, liquid intrusion and thermoporometry. *Part. Part. Syst. Char.*, 2004, **21**(2), 128–137.
44. Rouessac, V., Coustel, R., Bosc, F., Durand, J. and Ayral, A., Characterisation of mesostructured TiO_2 thin layers by ellipsometric porosimetry. *Thin Solid Films*, 2006, **495**(1/2), 232–236.
45. Tompkins, H. G. and Mc Gahan, W. A., *Spectroscopic Ellipsometry and Reflectometry: A User's Guide*. John Wiley and Sons, New York, 1999.
46. Yusuf, M. M., Imai, H. and Hirashima, H., Preparation of porous titania film by modified sol–gel method and its application to photocatalyst. *J. Sol–Gel Sci. Technol.*, 2002, **25**(1), 65–74.
47. Srikanth, K., Rahman, M. M., Tanaka, H., Krishna, K. M., Soga, T., Mishra, M. K. *et al.*, Investigation of the effect of sol processing parameters on the photoelectrical properties of dye-sensitized TiO_2 solar cells. *Sol. Energy Mater. Sol. Cells*, 2001, **65**(1–4), 171–177.
48. Truijen, I., Hardy, A., Van Bael, M. K., Van den Rul, H. and Mullens, J., Study of the decomposition of aqueous citratoperoxo-Ti(IV)-gel precursors for titania by means of TGA-MS and FTIR. *Thermochim. Acta*, 2007, **456**, 38–47.